

Longitudinal scaling property of the charge balance function in Au + Au collisions  
at  $\sqrt{s_{NN}} = 200$  GeV

B. I. Abelev,<sup>8</sup> M. M. Aggarwal,<sup>31</sup> Z. Ahammed,<sup>48</sup> A. V. Alakhverdyants,<sup>18</sup> I. Alekseev,<sup>16</sup> B. D. Anderson,<sup>19</sup>  
D. Arkhipkin,<sup>3</sup> G. S. Averichev,<sup>18</sup> J. Balewski,<sup>23</sup> L. S. Barnby,<sup>2</sup> S. Baumgart,<sup>53</sup> D. R. Beavis,<sup>3</sup> R. Bellwied,<sup>51</sup>  
M. J. Betancourt,<sup>23</sup> R. R. Betts,<sup>8</sup> A. Bhasin,<sup>17</sup> A. K. Bhati,<sup>31</sup> H. Bichsel,<sup>50</sup> J. Bielcik,<sup>10</sup> J. Bielcikova,<sup>11</sup> B. Biritz,<sup>6</sup>  
L. C. Bland,<sup>3</sup> B. E. Bonner,<sup>37</sup> J. Bouchet,<sup>19</sup> E. Braidot,<sup>28</sup> A. V. Brandin,<sup>26</sup> A. Bridgeman,<sup>1</sup> E. Bruna,<sup>53</sup>  
S. Bueltmann,<sup>30</sup> I. Bunzarov,<sup>18</sup> T. P. Burton,<sup>3</sup> X. Z. Cai,<sup>41</sup> H. Caines,<sup>53</sup> M. Calderón de la Barca Sánchez,<sup>5</sup>  
O. Catu,<sup>53</sup> D. Cebra,<sup>5</sup> R. Cendejas,<sup>6</sup> M. C. Cervantes,<sup>43</sup> Z. Chajecki,<sup>29</sup> P. Chaloupka,<sup>11</sup> S. Chattopadhyay,<sup>48</sup>  
H. F. Chen,<sup>39</sup> J. H. Chen,<sup>41</sup> J. Y. Chen,<sup>52</sup> J. Cheng,<sup>45</sup> M. Cherney,<sup>9</sup> A. Chikanian,<sup>53</sup> K. E. Choi,<sup>35</sup> W. Christie,<sup>3</sup>  
P. Chung,<sup>11</sup> R. F. Clarke,<sup>43</sup> M. J. M. Coddington,<sup>43</sup> R. Corliss,<sup>23</sup> J. G. Cramer,<sup>50</sup> H. J. Crawford,<sup>4</sup>  
D. Das,<sup>5</sup> S. Dash,<sup>13</sup> A. Davila Leyva,<sup>44</sup> L. C. De Silva,<sup>51</sup> R. R. Debbé,<sup>3</sup> T. G. Dedovich,<sup>18</sup> M. DePhillips,<sup>3</sup>  
A. A. Derevschikov,<sup>33</sup> R. Derradi de Souza,<sup>7</sup> L. Didenko,<sup>3</sup> P. Djawotho,<sup>43</sup> S. M. Dogra,<sup>17</sup> X. Dong,<sup>22</sup>  
J. L. Drachenberg,<sup>43</sup> J. E. Draper,<sup>5</sup> J. C. Dunlop,<sup>3</sup> M. R. Dutta Mazumdar,<sup>48</sup> L. G. Efimov,<sup>18</sup> E. Elhalhuli,<sup>2</sup>  
M. Elnimr,<sup>51</sup> J. Engelage,<sup>4</sup> G. Eppley,<sup>37</sup> B. Erazmus,<sup>42</sup> M. Estienne,<sup>42</sup> L. Eun,<sup>32</sup> O. Evdokimov,<sup>8</sup> P. Fachini,<sup>3</sup>  
R. Fatemi,<sup>20</sup> J. Fedorisin,<sup>18</sup> R. G. Fersch,<sup>20</sup> P. Filip,<sup>18</sup> E. Finch,<sup>53</sup> V. Fine,<sup>3</sup> Y. Fisyak,<sup>3</sup> C. A. Gagliardi,<sup>43</sup>  
D. R. Gangadharan,<sup>6</sup> M. S. Ganti,<sup>48</sup> E. J. Garcia-Solis,<sup>8</sup> A. Geromitsos,<sup>42</sup> F. Geurts,<sup>37</sup> V. Ghazikhanian,<sup>6</sup>  
P. Ghosh,<sup>48</sup> Y. N. Gorbunov,<sup>9</sup> A. Gordon,<sup>3</sup> O. Grebenyuk,<sup>22</sup> D. Grosnick,<sup>47</sup> B. Grube,<sup>35</sup> S. M. Guertin,<sup>6</sup>  
A. Gupta,<sup>17</sup> N. Gupta,<sup>17</sup> W. Guryon,<sup>3</sup> B. Haag,<sup>5</sup> A. Hamed,<sup>43</sup> L-X. Han,<sup>41</sup> J. W. Harris,<sup>53</sup> J. P. Hays-Wehle,<sup>23</sup>  
M. Heinz,<sup>53</sup> S. Heppelmann,<sup>32</sup> A. Hirsch,<sup>34</sup> E. Hjort,<sup>22</sup> A. M. Hoffman,<sup>23</sup> G. W. Hoffmann,<sup>44</sup> D. J. Hofman,<sup>8</sup>  
R. S. Hollis,<sup>8</sup> B. Huang,<sup>39</sup> H. Z. Huang,<sup>6</sup> T. J. Humanic,<sup>29</sup> L. Huo,<sup>43</sup> G. Igo,<sup>6</sup> A. Iordanova,<sup>8</sup> P. Jacobs,<sup>22</sup>  
W. W. Jacobs,<sup>15</sup> P. Jakl,<sup>11</sup> C. Jena,<sup>13</sup> F. Jin,<sup>41</sup> C. L. Jones,<sup>23</sup> P. G. Jones,<sup>2</sup> J. Joseph,<sup>19</sup> E. G. Judd,<sup>4</sup> S. Kabana,<sup>42</sup>  
K. Kajimoto,<sup>44</sup> K. Kang,<sup>45</sup> J. Kapitan,<sup>11</sup> K. Kauder,<sup>8</sup> D. Keane,<sup>19</sup> A. Kechechyan,<sup>18</sup> D. Kettler,<sup>50</sup> D. P. Kikola,<sup>22</sup>  
J. Kiryluk,<sup>22</sup> A. Kisiel,<sup>49</sup> S. R. Klein,<sup>22</sup> A. G. Knospe,<sup>53</sup> A. Kocoloski,<sup>23</sup> D. D. Koetke,<sup>47</sup> T. Kollegger,<sup>12</sup>  
J. Konzer,<sup>34</sup> M. Kopytine,<sup>19</sup> I. Koralt,<sup>30</sup> L. Koroleva,<sup>16</sup> W. Korsch,<sup>20</sup> L. Kotchenda,<sup>26</sup> V. Kouchpil,<sup>11</sup> P. Kravtsov,<sup>26</sup>  
K. Krueger,<sup>1</sup> M. Krus,<sup>10</sup> L. Kumar,<sup>31</sup> P. Kurnadi,<sup>6</sup> M. A. C. Lamont,<sup>3</sup> J. M. Landgraf,<sup>3</sup> S. LaPointe,<sup>51</sup> J. Lauret,<sup>3</sup>  
A. Lebedev,<sup>3</sup> R. Lednicky,<sup>18</sup> C-H. Lee,<sup>35</sup> J. H. Lee,<sup>3</sup> W. Leight,<sup>23</sup> M. J. LeVine,<sup>3</sup> C. Li,<sup>39</sup> L. Li,<sup>44</sup> N. Li,<sup>52</sup> W. Li,<sup>41</sup>  
X. Li,<sup>40</sup> X. Li,<sup>34</sup> Y. Li,<sup>45</sup> Z. M. Li,<sup>52</sup> G. Lin,<sup>53</sup> S. J. Lindenbaum,<sup>27</sup> \* M. A. Lisa,<sup>29</sup> F. Liu,<sup>52</sup> H. Liu,<sup>5</sup> J. Liu,<sup>37</sup>  
L. S. Liu,<sup>52</sup> \* T. Ljubicic,<sup>3</sup> W. J. Llope,<sup>37</sup> R. S. Longacre,<sup>3</sup> W. A. Love,<sup>3</sup> Y. Lu,<sup>39</sup> X. Luo,<sup>39</sup> G. L. Ma,<sup>41</sup>  
Y. G. Ma,<sup>41</sup> D. P. Mahapatra,<sup>13</sup> R. Majka,<sup>53</sup> O. I. Mall,<sup>5</sup> L. K. Mangotra,<sup>17</sup> R. Manweiler,<sup>47</sup> S. Margetis,<sup>19</sup>  
C. Markert,<sup>44</sup> H. Masui,<sup>22</sup> H. S. Matis,<sup>22</sup> Yu. A. Matulenko,<sup>33</sup> D. McDonald,<sup>37</sup> T. S. McShane,<sup>9</sup> A. Meschanin,<sup>33</sup>  
R. Milner,<sup>23</sup> N. G. Minaev,<sup>33</sup> S. Mioduszewski,<sup>43</sup> A. Mischke,<sup>28</sup> M. K. Mitrovski,<sup>12</sup> B. Mohanty,<sup>48</sup> M. M. Mondal,<sup>48</sup>  
B. Morozov,<sup>16</sup> D. A. Morozov,<sup>33</sup> M. G. Munhoz,<sup>38</sup> B. K. Nandi,<sup>14</sup> C. Nattrass,<sup>53</sup> T. K. Nayak,<sup>48</sup> J. M. Nelson,<sup>2</sup>  
P. K. Netrakanti,<sup>34</sup> M. J. Ng,<sup>4</sup> L. V. Nogach,<sup>33</sup> S. B. Nurushev,<sup>33</sup> G. Odyniec,<sup>22</sup> A. Ogawa,<sup>3</sup> H. Okada,<sup>3</sup>  
V. Okorokov,<sup>26</sup> D. Olson,<sup>22</sup> M. Pachr,<sup>10</sup> B. S. Page,<sup>15</sup> S. K. Pal,<sup>48</sup> Y. Pandit,<sup>19</sup> Y. Panebratsev,<sup>18</sup> T. Pawlak,<sup>49</sup>  
T. Peitzmann,<sup>28</sup> V. Perevoztchikov,<sup>3</sup> C. Perkins,<sup>4</sup> W. Peryt,<sup>49</sup> S. C. Phatak,<sup>13</sup> P. Pile,<sup>3</sup> M. Planinic,<sup>54</sup>  
M. A. Ploskon,<sup>22</sup> J. Pluta,<sup>49</sup> D. Plyku,<sup>30</sup> N. Poljak,<sup>54</sup> A. M. Poskanzer,<sup>22</sup> B. V. K. S. Potukuchi,<sup>17</sup> C. B. Powell,<sup>22</sup>  
D. Prindle,<sup>50</sup> C. Pruneau,<sup>51</sup> N. K. Pruthi,<sup>31</sup> P. R. Pujahari,<sup>14</sup> J. Putschke,<sup>53</sup> R. Raniwala,<sup>36</sup> S. Raniwala,<sup>36</sup>  
R. L. Ray,<sup>44</sup> R. Redwine,<sup>23</sup> R. Reed,<sup>5</sup> H. G. Ritter,<sup>22</sup> J. B. Roberts,<sup>37</sup> O. V. Rogachevskiy,<sup>18</sup> J. L. Romero,<sup>5</sup>  
A. Rose,<sup>22</sup> C. Roy,<sup>42</sup> L. Ruan,<sup>3</sup> R. Sahoo,<sup>42</sup> S. Sakai,<sup>6</sup> I. Sakrejda,<sup>22</sup> T. Sakuma,<sup>23</sup> S. Salur,<sup>5</sup> J. Sandweiss,<sup>53</sup>  
E. Sangaline,<sup>5</sup> J. Schambach,<sup>44</sup> R. P. Scharenberg,<sup>34</sup> N. Schmitz,<sup>24</sup> T. R. Schuster,<sup>12</sup> J. Seele,<sup>23</sup> J. Seger,<sup>9</sup>  
I. Selyuzhenkov,<sup>15</sup> P. Seyboth,<sup>24</sup> E. Shahaliev,<sup>18</sup> M. Shao,<sup>39</sup> M. Sharma,<sup>51</sup> S. S. Shi,<sup>52</sup> E. P. Sichtermann,<sup>22</sup>  
F. Simon,<sup>24</sup> R. N. Singaraju,<sup>48</sup> M. J. Skoby,<sup>34</sup> N. Smirnov,<sup>53</sup> P. Sorensen,<sup>3</sup> J. Sowinski,<sup>15</sup> H. M. Spinka,<sup>1</sup>  
B. Srivastava,<sup>34</sup> T. D. S. Stanislaus,<sup>47</sup> D. Staszak,<sup>6</sup> J. R. Stevens,<sup>15</sup> R. Stock,<sup>12</sup> M. Strikhanov,<sup>26</sup> B. Stringfellow,<sup>34</sup>  
A. A. P. Suaide,<sup>38</sup> M. C. Suarez,<sup>8</sup> N. L. Subba,<sup>19</sup> M. Sumbera,<sup>11</sup> X. M. Sun,<sup>22</sup> Y. Sun,<sup>39</sup> Z. Sun,<sup>21</sup> B. Surrow,<sup>23</sup>  
D. N. Svirida,<sup>16</sup> T. J. M. Symons,<sup>22</sup> A. Szanto de Toledo,<sup>38</sup> J. Takahashi,<sup>7</sup> A. H. Tang,<sup>3</sup> Z. Tang,<sup>39</sup>  
L. H. Tarini,<sup>51</sup> T. Tarnowsky,<sup>25</sup> D. Thein,<sup>44</sup> J. H. Thomas,<sup>22</sup> J. Tian,<sup>41</sup> A. R. Timmins,<sup>51</sup> S. Timoshenko,<sup>26</sup>  
D. Tlusty,<sup>11</sup> M. Tokarev,<sup>18</sup> T. A. Trainor,<sup>50</sup> V. N. Tram,<sup>22</sup> S. Trentalange,<sup>6</sup> R. E. Tribble,<sup>43</sup> O. D. Tsai,<sup>6</sup>  
J. Ulery,<sup>34</sup> T. Ullrich,<sup>3</sup> D. G. Underwood,<sup>1</sup> G. Van Buren,<sup>3</sup> M. van Leeuwen,<sup>28</sup> G. van Nieuwenhuizen,<sup>23</sup>  
J. A. Vanfossen, Jr.,<sup>19</sup> R. Varma,<sup>14</sup> G. M. S. Vasconcelos,<sup>7</sup> A. N. Vasiliev,<sup>33</sup> F. Videbaek,<sup>3</sup> Y. P. Viyogi,<sup>48</sup>  
S. Vokal,<sup>18</sup> S. A. Voloshin,<sup>51</sup> M. Wada,<sup>44</sup> M. Walker,<sup>23</sup> F. Wang,<sup>34</sup> G. Wang,<sup>6</sup> H. Wang,<sup>25</sup> J. S. Wang,<sup>21</sup>  
Q. Wang,<sup>34</sup> X. L. Wang,<sup>39</sup> Y. Wang,<sup>45</sup> G. Webb,<sup>20</sup> J. C. Webb,<sup>3</sup> G. D. Westfall,<sup>25</sup> C. Whitten Jr.,<sup>6</sup> H. Wieman,<sup>22</sup>  
E. Wingfield,<sup>44</sup> S. W. Wissink,<sup>15</sup> R. Witt,<sup>46</sup> Y. F. Wu,<sup>52</sup> W. Xie,<sup>34</sup> N. Xu,<sup>22</sup> Q. H. Xu,<sup>40</sup> W. Xu,<sup>6</sup> Y. Xu,<sup>39</sup>

Z. Xu,<sup>3</sup> L. Xue,<sup>41</sup> Y. Yang,<sup>21</sup> P. Yepes,<sup>37</sup> K. Yip,<sup>3</sup> I-K. Yoo,<sup>35</sup> Q. Yue,<sup>45</sup> M. Zawisza,<sup>49</sup> H. Zbroszczyk,<sup>49</sup> W. Zhan,<sup>21</sup> J. Zhang,<sup>52</sup> S. Zhang,<sup>41</sup> W. M. Zhang,<sup>19</sup> X. P. Zhang,<sup>22</sup> Y. Zhang,<sup>22</sup> Z. P. Zhang,<sup>39</sup> J. Zhao,<sup>41</sup> C. Zhong,<sup>41</sup> J. Zhou,<sup>37</sup> W. Zhou,<sup>40</sup> X. Zhu,<sup>45</sup> Y. H. Zhu,<sup>41</sup> R. Zoukarnneev,<sup>18</sup> and Y. Zoukarnneeva<sup>18</sup>

(STAR Collaboration)

- <sup>1</sup>Argonne National Laboratory, Argonne, Illinois 60439, USA  
<sup>2</sup>University of Birmingham, Birmingham, United Kingdom  
<sup>3</sup>Brookhaven National Laboratory, Upton, New York 11973, USA  
<sup>4</sup>University of California, Berkeley, California 94720, USA  
<sup>5</sup>University of California, Davis, California 95616, USA  
<sup>6</sup>University of California, Los Angeles, California 90095, USA  
<sup>7</sup>Universidade Estadual de Campinas, Sao Paulo, Brazil  
<sup>8</sup>University of Illinois at Chicago, Chicago, Illinois 60607, USA  
<sup>9</sup>Creighton University, Omaha, Nebraska 68178, USA  
<sup>10</sup>Czech Technical University in Prague, FNSPE, Prague, 115 19, Czech Republic  
<sup>11</sup>Nuclear Physics Institute AS CR, 250 68 Řež/Prague, Czech Republic  
<sup>12</sup>University of Frankfurt, Frankfurt, Germany  
<sup>13</sup>Institute of Physics, Bhubaneswar 751005, India  
<sup>14</sup>Indian Institute of Technology, Mumbai, India  
<sup>15</sup>Indiana University, Bloomington, Indiana 47408, USA  
<sup>16</sup>Alikhanov Institute for Theoretical and Experimental Physics, Moscow, Russia  
<sup>17</sup>University of Jammu, Jammu 180001, India  
<sup>18</sup>Joint Institute for Nuclear Research, Dubna, 141 980, Russia  
<sup>19</sup>Kent State University, Kent, Ohio 44242, USA  
<sup>20</sup>University of Kentucky, Lexington, Kentucky, 40506-0055, USA  
<sup>21</sup>Institute of Modern Physics, Lanzhou, China  
<sup>22</sup>Lawrence Berkeley National Laboratory, Berkeley, California 94720, USA  
<sup>23</sup>Massachusetts Institute of Technology, Cambridge, MA 02139-4307, USA  
<sup>24</sup>Max-Planck-Institut für Physik, Munich, Germany  
<sup>25</sup>Michigan State University, East Lansing, Michigan 48824, USA  
<sup>26</sup>Moscow Engineering Physics Institute, Moscow Russia  
<sup>27</sup>City College of New York, New York City, New York 10031, USA  
<sup>28</sup>NIKHEF and Utrecht University, Amsterdam, The Netherlands  
<sup>29</sup>Ohio State University, Columbus, Ohio 43210, USA  
<sup>30</sup>Old Dominion University, Norfolk, VA, 23529, USA  
<sup>31</sup>Panjab University, Chandigarh 160014, India  
<sup>32</sup>Pennsylvania State University, University Park, Pennsylvania 16802, USA  
<sup>33</sup>Institute of High Energy Physics, Protvino, Russia  
<sup>34</sup>Purdue University, West Lafayette, Indiana 47907, USA  
<sup>35</sup>Pusan National University, Pusan, Republic of Korea  
<sup>36</sup>University of Rajasthan, Jaipur 302004, India  
<sup>37</sup>Rice University, Houston, Texas 77251, USA  
<sup>38</sup>Universidade de Sao Paulo, Sao Paulo, Brazil  
<sup>39</sup>University of Science & Technology of China, Hefei 230026, China  
<sup>40</sup>Shandong University, Jinan, Shandong 250100, China  
<sup>41</sup>Shanghai Institute of Applied Physics, Shanghai 201800, China  
<sup>42</sup>SUBATECH, Nantes, France  
<sup>43</sup>Texas A&M University, College Station, Texas 77843, USA  
<sup>44</sup>University of Texas, Austin, Texas 78712, USA  
<sup>45</sup>Tsinghua University, Beijing 100084, China  
<sup>46</sup>United States Naval Academy, Annapolis, MD 21402, USA  
<sup>47</sup>Valparaiso University, Valparaiso, Indiana 46383, USA  
<sup>48</sup>Variable Energy Cyclotron Centre, Kolkata 700064, India  
<sup>49</sup>Warsaw University of Technology, Warsaw, Poland  
<sup>50</sup>University of Washington, Seattle, Washington 98195, USA  
<sup>51</sup>Wayne State University, Detroit, Michigan 48201, USA  
<sup>52</sup>Institute of Particle Physics, CCNU (HZNU), Wuhan 430079, China  
<sup>53</sup>Yale University, New Haven, Connecticut 06520, USA  
<sup>54</sup>University of Zagreb, Zagreb, HR-10002, Croatia

(Dated: October 15, 2018)

We present measurements of the charge balance function, from the charged particles, for diverse pseudorapidity and transverse momentum ranges in Au + Au collisions at  $\sqrt{s_{NN}} = 200$  GeV using the STAR detector at RHIC. We observe that the balance function is boost-invariant within

the pseudorapidity coverage  $[-1.3, 1.3]$ . The balance function properly scaled by the width of the observed pseudorapidity window does not depend on the position or size of the pseudorapidity window. This scaling property also holds for particles in different transverse momentum ranges. In addition, we find that the width of the balance function decreases monotonically with increasing transverse momentum for all centrality classes.

PACS numbers: 13.85.Hd, 25.75.Gz

Particle production in elementary collisions at high energy is constrained by conservation laws. Electric charge conservation, in particular, constrains the balance of charged particles produced in a collision. The electric charge balance function (BF) is an observable specifically designed to measure the balance, and thereby provide insight into the particle production processes in elementary collisions at high energy [1]. It has been used in hadron-hadron, lepton-hadron, and  $e^+e^-$  collisions to study hadronization schemes [1–3]. The BF has recently gained particular interest in clocking hadronization in relativistic heavy-ion collisions, where a new state of matter - the quark-gluon plasma (QGP) - would be formed. The formation of QGP will allow a partonic charge diffusion in longitudinal phase space, and would lead to a widening of the charge balance function [4].

The BF is defined in terms of a combination of four different conditional densities of charged hadrons [1]. It measures how the net charge at any point of the phase space is rearranged if the charge at a selected point changes. Projected on to the pseudorapidity difference  $\delta\eta = \eta_1 - \eta_2$  of two charged particles in a given pseudorapidity window  $\eta_w$ , the BF becomes [4, 5]

$$B(\delta\eta|\eta_w) = \frac{1}{2} \left[ \frac{\langle n_{+-}(\delta\eta, \eta_w) \rangle - \langle n_{++}(\delta\eta, \eta_w) \rangle}{\langle n_+(\eta_w) \rangle} + \frac{\langle n_{-+}(\delta\eta, \eta_w) \rangle - \langle n_{--}(\delta\eta, \eta_w) \rangle}{\langle n_-(\eta_w) \rangle} \right] \quad (1)$$

where  $\langle n_+(\eta_w) \rangle$  and  $\langle n_-(\eta_w) \rangle$  are respectively the event averaged number of measured positively and negatively charged particles.  $\langle n_{+-}(\delta\eta, \eta_w) \rangle = \langle n_{-+}(\delta\eta, \eta_w) \rangle$  is the event averaged number of pairs of particles with opposite charges separated by pseudorapidity  $\delta\eta$ .  $\langle n_{++}(\delta\eta, \eta_w) \rangle$  and  $\langle n_{--}(\delta\eta, \eta_w) \rangle$  are defined correspondingly for pairs of positively and negatively charged particles, respectively. The charge balance function is a differential combination of all possible charge correlations. Its integral over rapidity space is related to measures of charge fluctuation [6].

Measurements of the BF in relativistic heavy-ion collisions have been reported by several experiments [5, 7, 8]. However, these experiments feature significant difference of acceptance in pseudorapidity and transverse momentum. Comparison of results from these experiments is thus only qualitative. A quantitative comparative analysis of these results requires a better understanding of

the BF dependence on pseudorapidity and momentum acceptance [5, 7, 9, 10].

This BF dependence has been studied in  $\pi^+p$  and  $K^+p$  collisions at 250 GeV/c incident beam momentum by a fixed target experiment with large acceptance [9]. In those collisions, the BF is found to be invariant under longitudinal boost over the whole rapidity range of produced particles ( $-5 < y < 5$ ), i.e., the ratio of  $B(\delta y|y_w)$  to  $(1 - \delta y/|y_w|)$  is independent of the observed window,  $|y_w|$ , and corresponds to the BF of the whole rapidity range.

The aim of the analysis presented in this paper is to verify whether the boost invariance observed in elementary collisions is also present in Au + Au collisions at  $\sqrt{s_{NN}} = 200$  GeV. To this end, we first study the BF using equal size pseudorapidity windows spanning various pseudorapidity ranges within a relatively wide pseudorapidity coverage of the STAR Time Projection Chamber (TPC). Given that the shape of the BF depends by definition on the width of the pseudorapidity acceptance, we next scale the measured BF by an acceptance factor determined by the width of the observed pseudorapidity window. The scaled balance function,  $B_s(\delta\eta)$ , is defined as

$$B_s(\delta\eta) = \frac{B(\delta\eta|\eta_w)}{1 - \frac{\delta\eta}{|\eta_w|}} \quad (2)$$

where  $\delta\eta$  is the particle separation in pseudorapidity, and  $|\eta_w|$  represents the size of pseudorapidity window. This scaled BF shows how the balance function extends with the widening of the pseudorapidity window.

We further explore the scaling property of the BF in different ranges of transverse momentum  $p_T$ . The  $p_T$  of final state particles is suggested to characterize their emission proper-time  $\tau$  [11–13]. Particles with different  $p_T$  may be produced at different stages of the evolution after the collision. This relation between  $p_T$  and  $\tau$  has been assumed in hydrodynamic models [14], which qualitatively describe the data of  $p_T$  dependence of anisotropic collective flow [15]. Examining the  $p_T$  dependence of the scaling of the BF will provide an additional experimental test of this assumption.

In thermal models, particle velocities are determined by the local temperature, collective flow velocity and the particle masses. For relativistic particles, the thermal velocity along the beam axis is a function of the particle's transverse mass, and therefore is affected by transverse expansion. Lower freeze-out temperature and/or larger transverse mass of higher  $p_T$  particles are expected to

---

\*Deceased

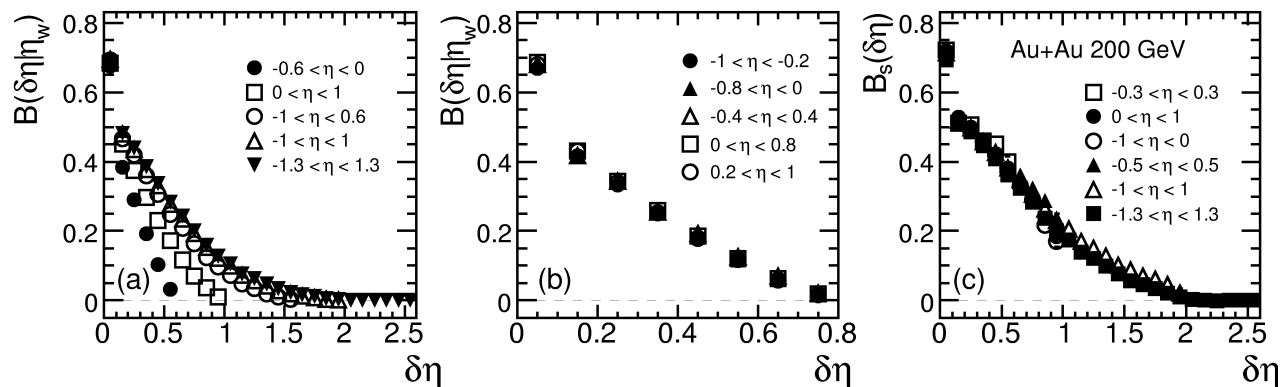


FIG. 1: (a) Balance functions in five pseudorapidity windows of different width; (b) Balance functions observed at five different positions of pseudorapidity windows with  $|\eta_w| = 0.8$ ; (c) Scaled balance function,  $B_s(\delta\eta)$ , obtained for various pseudorapidity window widths and positions. The data are from 0–80% Au+Au collisions at 200 GeV and the particle  $p_T$  range is  $0.15 < p_T < 2$  GeV/c. Statistical errors are smaller than the symbol sizes. Systematic errors are of the order of 5%.

result in smaller thermal velocity in the longitudinal direction and narrower BF [4, 6].

In this letter, we first give brief descriptions of the analysis parameters and techniques. We then present measurements of the BF, and its dependence on the width of the pseudorapidity window. We test the boost-invariance of the BF, i.e. verify whether it is independent of the position of same-width pseudorapidity windows. We next examine the universality of the scaled BF. Finally, the scaling property of the BF for particles within different transverse momentum ranges is studied.

Our BF analysis is restricted to charged particles measured within the STAR TPC detector [16]. This detector is well suited for precise studies of correlation structures given its relatively wide pseudorapidity range  $-1.3 < \eta < 1.3$  and full azimuthal acceptance. Recorded events were selected on the basis of a minimum-bias trigger defined by the coincidence of two zero-degree calorimeters (ZDCs) [17] located at  $\pm 18$  m from the center of the TPC. Events are further required to have a primary vertex position within 25 cm, longitudinally, of the TPC center and within 1 cm, radially, of the beam line. This analysis is restricted to charged particle tracks in the  $p_T$  range  $0.15 < p_T < 2.0$  GeV/c. After all these cuts, 5.7 million minimum-bias events were selected for the analysis. Tracks are required to pass within 2 cm of the primary vertex in order to reduce weak-decay contributions. Tracks are further required to consist of a minimum of 15 measured points and have a ratio of the numbers of measured to possible points larger than 0.52 to avoid track splitting effects. These two cuts minimize detector and track reconstruction effects, such as ghost tracks, track splitting, and enable optimal momentum resolution.

Figure 1(a) displays balance function obtained with five different pseudorapidity windows, located at various positions, and with sizes ranging from  $|\eta_w| = 0.6$  to 2.6. It shows that the BF is strongly dependent on the width of the pseudorapidity window. Vertical bars shown in this

and following figures indicate statistical errors only. Statistical errors are smaller than the symbol sizes in Fig. 1. Systematic errors are of the order of 5% and due to uncertainties in the track reconstruction efficiency associated with the track cuts, and event-by-event variations of the vertex position.

In order to test directly whether the BF is boost-invariant under longitudinal translation within the STAR TPC, we examine, in Fig. 1(b), five BFs measured in equal size ( $|\eta_w| = 0.8$ ) pseudorapidity windows located at different positions. One observes that the five BFs overlap with one another thereby indicating that the BF is independent of the position of the pseudorapidity window, i.e.,  $B(\delta\eta|\eta_w)$  is invariant under a longitudinal translation within the range  $-1 < \eta < 1$ . Note that the large BF values measured at  $\delta\eta = 0.01$  arise in part from HBT and Coulomb effects [5, 6]. We also considered five equal size and non-overlapping windows, not shown in Fig. 1, and found similar agreements.

In Fig. 1(c), we present scaled balance functions,  $B_s$ , calculated with Eq. 2, obtained from BFs measured with four distinct pseudorapidity window widths ( $|\eta_w| = 0.6, 1, 2, 2.6$ ) and six window positions. We find that the scaled balance functions have equal shape and magnitude, and are identical within experimental errors. Therefore  $B_s$  is independent of the size and position of the window  $\eta_w$  in the pseudorapidity range  $-1 < \eta < 1$ . A similar invariance of  $B_s$  was observed in hadron-hadron interactions over the whole rapidity range of produced particles [9].

Lastly, we investigate whether the scaling property of the BF holds for particles in different  $p_T$  ranges and study how the width of the BF changes with  $p_T$ . Figure 2 displays scaled balance function obtained for four  $p_T$  ranges: (0.15, 0.4), (0.4, 0.7), (0.7, 1) and (1, 2) GeV/c, and the same pseudorapidity windows as used in Fig. 1 (c). We find that the distributions measured in specific  $p_T$  intervals are independent of the size and position of the pseudorapidity window used to carry out the measurement.



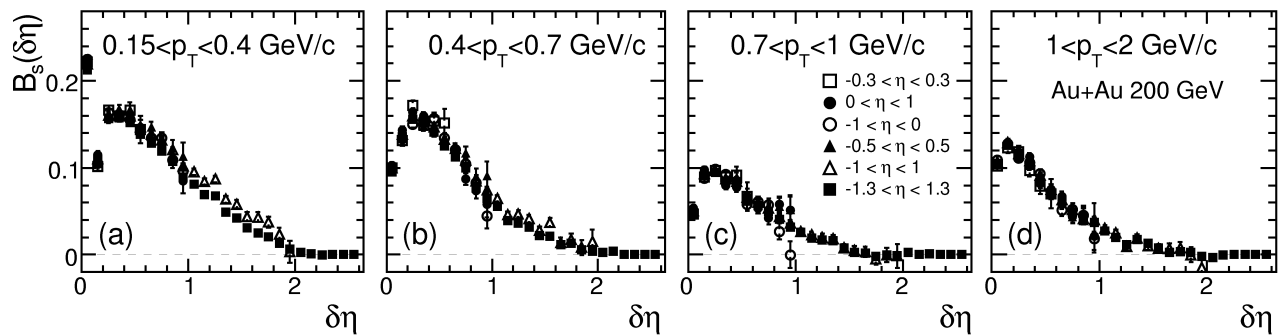


FIG. 2:  $B_s(\delta\eta)$  based on  $B(\delta\eta|\eta_w)$  values measured in different pseudorapidity windows for particles in four  $p_T$  bins. The data are from 0 – 80% Au+Au collisions at 200 GeV. Error bars are statistical only. Systematic errors are of the order of 5%.

We thus conclude that the invariance of  $B_s$  observed for  $0.15 < p_T < 2.0$  GeV/c also holds for small transverse momentum ranges.

Comparing the distributions shown in Fig. 2(a) to 2(d), we observe that the scaled balance function,  $B_s(\delta\eta)$ , changes significantly in shape and amplitude with the transverse-momentum of final state particles. The widths of  $B_s(\delta\eta)$  defined as [5]

$$\langle \delta\eta \rangle = \frac{\sum_i B_s(\delta\eta_i) \delta\eta_i}{\sum_i B_s(\delta\eta_i)} \quad (3)$$

are presented in Table I. The first data point in Fig. 2(a) is affected by HBT correlations, which result in a strong correlation at small relative  $p_T$ . On the other hand, track merging effects deplete the balance function at small  $\delta\eta$ . To assess the systematic uncertainties on the extracted width, we use extrapolated values for the data points at the two lowest  $\delta\eta$  instead of their measured ones in calculating the width. For the lower bound of systematic uncertainty estimate, the extrapolations from the larger  $\delta\eta$  data are done by two functional forms in order to well fit the data. One is exponential for the  $p_T$  in (0.15, 0.4) GeV/c and Gaussian for the other three  $p_T$  bins. For the upper bound of systematic uncertainty estimate, the extrapolated function is multinomial for all four  $p_T$  bins. Table I shows that the width of the scaled BF becomes narrower for increasing  $p_T$ . This observation is qualitatively consistent with expectations from thermal models [6].

As shown in [5], the width of the BF decreases with collision centrality. The decreases in the BF width with increasing  $p_T$  and increasing centrality could be associated with transverse radial flow [18]. In order to disentangle these effects, we further study the  $p_T$  dependence of  $\langle \delta\eta \rangle$  in different centrality bins. This is shown in the upper panel of Fig. 3. It shows clearly that the width of the BF decreases with increasing transverse momentum of final state particles in each centrality bin. We also study the centrality dependence of  $\langle \delta\eta \rangle$  in different  $p_T$  intervals. This is presented in the lower panel of Fig. 3. It shows that the narrowing of the BF with increasing centrality is present in all  $p_T$  bins. Our results demonstrate that the

BF becomes narrower with increasing  $p_T$  in each given centrality bin, and in more central collisions in each given  $p_T$  bin. The width of BF depends on both centrality and  $p_T$ . The origin of these narrowings and their possible connections should provide more insight into the particle production dynamics in relativistic heavy-ion collisions.

In summary, we present a first measurement of the longitudinal scaling property of the charge balance function in Au + Au collisions at 200 GeV with the STAR detector at RHIC. The results demonstrate that within the pseudorapidity range  $-1.3 < \eta < 1.3$ , the balance function in equal size windows is independent of the position of the window, and the balance function, when properly scaled by the width of the pseudorapidity window, is found to be independent of the position and size of the window. This scaling property of the balance function is also observed for particles in different  $p_T$  ranges. It is further shown that the width of the scaled BF decreases with increases of both the particle transverse momentum and the collision centrality. We conclude that the scaling property of the BF, observed in hadron-hadron collisions [9], is also present in nucleus-nucleus collisions at mid-rapidity at RHIC. This longitudinal property of BF provides a good test for the hadronization mechanism in currently available models [19]. The narrowing of the BF with increasing  $p_T$  and centrality warrants further investigation.

We thank Dr. Xin-Nian Wang for discussions on the scaling behavior of the charge balance function. We thank the RHIC Operations Group and RCF at BNL, the NERSC Center at LBNL and the Open Science Grid consortium for providing resources and support. This work was supported in part by the Offices of NP and HEP within the U.S. DOE Office of Science, the U.S. NSF, the Sloan Foundation, the DFG cluster of excellence ‘Origin and Structure of the Universe’ of Germany, CNRS/IN2P3, STFC and EPSRC of the United Kingdom, FAPESP CNPq of Brazil, Ministry of Ed. and Sci. of the Russian Federation, NNSFC, CAS, MoST, and MoE of China, GA and MSMT of the Czech Republic, FOM and NWO of the Netherlands, DAE, DST, and CSIR of India, Polish Ministry of Sci. and Higher Ed.,

TABLE I: The widths  $\langle\delta\eta\rangle$  of the  $B_s(\delta\eta)$  for four  $p_T$  bins. The first and second errors are statistical and systematic, respectively. The data are from 0 – 80% Au+Au collisions at 200 GeV.

$p_T(\text{GeV}/c)$	(0.15, 0.4)	(0.4, 0.7)	(0.7, 1)	(1, 2)
$\langle\delta\eta\rangle$	$0.652 \pm 0.006^{+0.081}_{-0.029}$	$0.609 \pm 0.008^{+0.049}_{-0.037}$	$0.536 \pm 0.016^{+0.047}_{-0.041}$	$0.487 \pm 0.014^{+0.079}_{-0.021}$

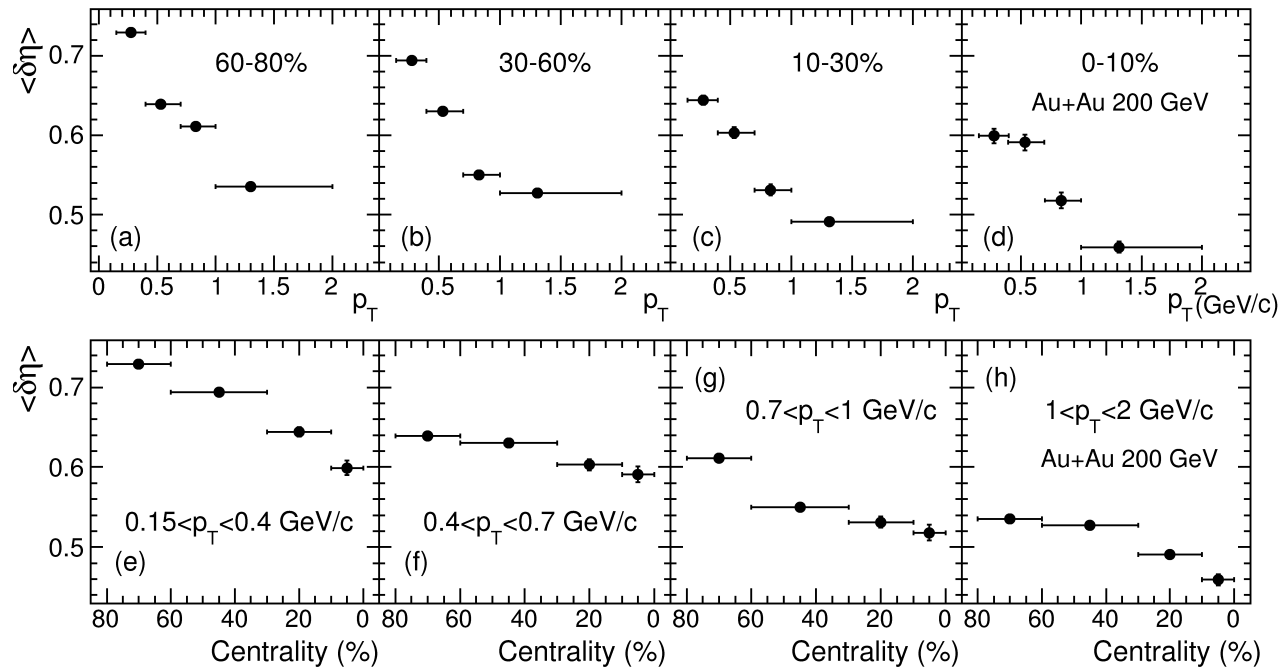


FIG. 3: Upper panel: the  $p_T$  dependence of the width of the BF in different centrality bins; Lower panel: the centrality dependence of the width of the BF in different  $p_T$  intervals. Data are from Au + Au collisions at 200 GeV.

Korea Research Foundation, Ministry of Sci., Ed. and Sports of the Rep. Of Croatia, Russian Ministry of Sci.

and Tech, and RosAtom of Russia.

- 
- [1] D. Drijard, et al., Nucl. Phys. B 166 (1980) 233; *ibid*, 155 (1979) 269.
- [2] P.D. Acton, et al., Phys. Lett. B 305 (1993) 415; M. Arneodo, et al., Z. Phys. C 36 (1987) 527.
- [3] R. Brandelik, et al., Phys. Lett. B 100 (1981) 357; M. Althoff, et al., Z. Phys. C 17 (1983) 5; H. Aihara, et al., Phys. Rev. Lett. 53 (1984) 2199 and 57 (1986) 3140.
- [4] S.A. Bass, P. Danielewicz, S. Pratt, Phys. Rev. Lett. 85 (2000) 2689.
- [5] J. Adams, et al., STAR Collaboration, Phys. Rev. Lett. 90 (2003) 172301; G.D. Westfall (for STAR Collaboration), J. Phys. G 30 (2004) S345.
- [6] S. Jeon, S. Pratt, Phys. Rev. C 65 (2002) 044902.
- [7] C. Alt, et al., NA49 Collaboration, Phys. Rev. C 71 (2005) 034903.
- [8] K. Adcox, et al., PHENIX Collaboration, Phys. Rev. Lett. 89 (2002) 082301.
- [9] M.R. Atayan, et al., NA22 Collaboration, Phys. Lett. B 637 (2006) 39.
- [10] T.A. Trainor, hep-ph/0301122.
- [11] R.C. Hwa, Y. Wu, Phys. Rev. C 60 (1999) 054904.
- [12] M. Asakawa, S.A. Bass, B. Müller, C. Nonaka, Phys. Rev. Lett. 101 (2008) 122302.
- [13] F. Grassi, Y. Hama, T. Kodama, Phys. Lett. B 355 (1995) 9; Y.M. Sinyukov, S.V. Akkelin, Y. Hama, Phys. Rev. Lett. 89 (2002) 052301;
- [14] P. Huovinen, P.F. Kolb, U. Heinz, P.V. Ruuskanen, S.A. Voloshin, Phys. Lett. B 503 (2001) 58.
- [15] J. Adams, et al., STAR Collaboration, Nucl. Phys. A 757 (2005) 102.
- [16] M. Anderson, et al., Nucl. Instrum. Meth. A 499 (2003) 659.
- [17] C. Adler, et al., Nucl. Instrum. Meth. A 461 (2001) 337.
- [18] S.A. Bass, P. Danielewicz, S. Pratt, Phys. Rev. Lett. 85 (2000) 2689; S. Pratt, S. Cheng, Phys. Rev. C 68 (2003) 014907; S.A. Voloshin, Phys. Lett. B 632 (2006) 490.
- [19] N. Li, Z. M. Li, Y. F. Wu, Phys. Rev. C 80 (2009) 064910.